

## Pre-collision evolution of the Piñón oceanic terrane of SW Ecuador: stratigraphy and geochemistry of the “Calentura Formation”

JEREMIE VAN MELLE<sup>1</sup>, WASHINGTON VILEMA<sup>2</sup>, BASTIEN FAURE-BRAC<sup>1</sup>, MARTHA ORDOÑEZ<sup>2</sup>, HENRIETTE LAPIERRE<sup>†</sup>, NELSON JIMENEZ<sup>2</sup>, ETIENNE JAILLARD<sup>1,3</sup> and MILTON GARCIA<sup>2</sup>

*Key-words.* – Stratigraphy, Late Cretaceous, Petrography, Geochemistry, Geodynamics, Ecuador.

*Abstract.* – The stratigraphic revision of the southern coastal Ecuadorian series makes possible the reconstruction of the pre-collision history of the Caribbean plateau accreted to the Ecuadorian margin. The Coniacian age of the oceanic basement (Piñón Fm) indicates that the latter is part of the Caribbean oceanic plateau. It is overlain by the Calentura Fm, which comprises from base to top: (i) 20 to 200 m of lavas and volcanic breccias of arc affinity (Las Orquídeas Mb), (ii) siliceous, organic rich black limestones of (middle?) Coniacian age, (iii) red, radiolarian rich, calcareous cherts ascribed to the Santonian-early Campanian, and (iv) marls, greywackes and island arc tuffs of Mid Campanian age. The latter are overlain by volcanoclastic turbidites of Mid to Late Campanian age (Cayo Fm), coeval to the Campanian-Maastrichtian island arc series located farther west (San Lorenzo Fm).

The Las Orquídeas magmatic unit is interpreted as resulting from the melting of the Caribbean plateau, rather than from an ephemeral subduction process. The transition from coniacian limestones to santonian red cherts would be related to the thermal subsidence of the Caribbean plateau. The uplift of the latter and the development of the San Lorenzo island arc in the Middle Campanian would be due to the collision of the Caribbean plateau with the Mexican margin. Early in the Late Maastrichtian, the collision of the Caribbean plateau with the Ecuadorian margin would have triggered the cessation of the San Lorenzo arc activity. In the Late Paleocene, the Caribbean plateau was split into two terranes: the western Piñón terrane, which collided with the eastern Guaranda terrane.

## Evolution pré-accrétion de l'unité océanique Piñón du Sud-Ouest de l'Équateur : Stratigraphie et géochimie de la “Formation Calentura”

*Mots-clés.* – Stratigraphie, Crétacé supérieur, Pétrographie, Géochimie, Géodynamique, Équateur.

*Résumé.* – La révision stratigraphique des séries crétacées de la côte sud-équatorienne permet de préciser les principales étapes de l'histoire pré-accrétion du plateau Caraïbe accrété à la marge équatorienne. L'âge coniacien du substratum océanique (Fm Piñón) montre qu'il appartient au plateau océanique Caraïbe. Il est surmonté par la Fm Calentura, constituée, de bas en haut, par (i) 20 à 200 m de laves et brèches volcaniques à signature d'arc (Mb Las Orquídeas), (ii) des calcaires siliceux riches en matière organique datés du Coniacien (moyen ?), (iii) des cherts rouges calcaires à radiolaires attribués au Santonien-Campanien inférieur, et (iv) des marnes, grauwwackes et tufs à géochimie d'arc, d'âge campanien moyen. Ceux-ci sont surmontés par des turbidites volcano-clastiques datées du Campanien moyen et supérieur (Fm Cayo), équivalentes des laves de l'arc insulaire campano-maastrichtien situé plus à l'ouest (Fm San Lorenzo).

Le magmatisme du Mb Las Orquídeas est interprété comme issu, non d'une subduction éphémère, mais de la fusion du plateau caraïbe encore chaud. Le passage des calcaires coniaciens aux cherts santoniens serait lié à la subsidence thermique du plateau Caraïbe. La surrection du plateau Caraïbe et la naissance de l'arc insulaire San Lorenzo au Campanien moyen, pourraient être liées à la collision du plateau Caraïbe avec la marge du Mexique. La collision du plateau Caraïbe avec la marge équatorienne au début du Maastrichtien supérieur provoquerait la fin de l'activité de l'arc insulaire San Lorenzo. Au Paléocène supérieur, le plateau Caraïbe se scinde en deux, le terrain occidental (Piñón) se trouvant sous-charrié sous le terrain oriental (Guaranda).

## INTRODUCTION

In contrast to the central Andes, the northern Andes (Ecuador, Colombia) include oceanic terranes accreted to the western part of the continental margin [Gansser, 1973; Gossens and Rose, 1973]. Geochemical studies demonstrated that these terranes are made of Cretaceous oceanic plateaus, often associated with Late Cretaceous to Paleogene island

arcs [Kerr *et al.*, 1996; Reynaud *et al.*, 1999; Mamberti *et al.*, 2003; 2004], accreted to the margin between Late Cretaceous and Paleogene times. The western Cordillera of central Ecuador comprises the western Macuchi terrane, and the eastern Pallatanga terrane, in turn subdivided into the Guaranda and San Juan terranes [e.g. Kerr *et al.*, 2002; Mamberti *et al.*, 2003, 2004; Jaillard *et al.*, 2004] (fig. 1), whereas the coast of southern Ecuador is floored by the

1. Univ. Joseph Fourier Grenoble 1, LGCA, UMR-CNRS 5025, Maison Géosciences, BP 53, F-38041 Grenoble cedex 9.

2. Petroproducción, Centro de Investigaciones Geológicas-Guayaquil, km 6,5 vía a la Costa, Guayaquil, Ecuador. cigg@telcel.net

3. Univ. Paul Sabatier Toulouse 1, IRD-UR 154, LMTG, 14 av. Edouard Belin, F-31400 Toulouse. Etienne.Jaillard@ujf-grenoble.fr

Manuscrit déposé le 4 mai 2007; accepté après révision le 24 septembre 2007

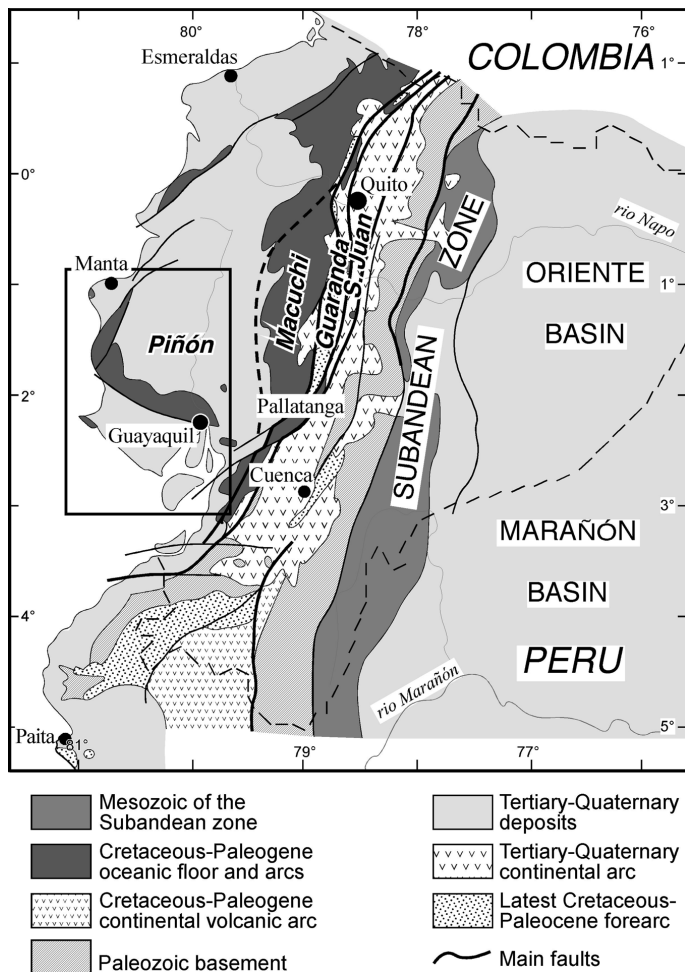


FIG. 1. – Structural sketch map of Ecuador.  
FIG. 1. – Schéma structural de l'Équateur.

Piñón Formation [Baldock, 1982]. Although most of the current debates focus on the number, age, and accretion history of these oceanic terranes [e.g. Jaillard *et al.*, 2004; Kerr and Tarney, 2005; Luzieux *et al.*, 2006 and references therein], little is known about the intra-oceanic, pre-accretion history of these units, and therefore, about the origin and early geodynamical evolution of these exotic terranes.

The aim of this work is to propose a reconstruction of the pre-accretion evolution of the Piñón oceanic plateau, which is well exposed in southwestern coastal Ecuador (Cordillera Chongón-Colonche, fig. 1 and 2). For this purpose, we tried to refine the stratigraphy and geodynamic significance of the sedimentary and magmatic bodies emplaced in the early Late Cretaceous.

## PREVIOUS WORKS

The Piñón Formation, made mainly of basalts and shallow level basic intrusions, was defined as the magmatic basement of the whole southern coastal Ecuador [Baldock, 1982]. This unit was previously referred to as the Basic Igneous Complex, of Early to Middle Cretaceous age [Goossens and Rose, 1973; Goossens *et al.*, 1977], whereas Olsson [1942] defined the Cayo Formation as the clastic

series overlying the Piñón Formation. Thalmann [1946] studied the sediments overlying the Piñón Formation, and identified:

- a fine-grained, silicified lower part, as the Calentura Member of Cenomanian-Turonian age,
- a thick clastic unit named the Cayo Formation,
- an upper cherty, fine-grained unit, referred to as the Guayaquil Formation of Maastrichtian age.

The Calentura Formation has been ascribed successively to the Cenomanian-Turonian [Thalmann, 1946], Turonian or younger [Bristow, 1976], and late Turonian-Coniacian or younger [Marksteiner and Alemán, 1991].

The poorly dated Cayo Formation has been assigned to the Late Cretaceous [Thalmann, 1946], Maastrichtian to Paleocene [Sigal, 1969; Faucher and Savoyat, 1973] and Maastrichtian to Middle Paleocene [Marksteiner and Alemán, 1991].

Farther west (Manta area), Lebrat *et al.* [1987] defined a late Cretaceous island arc, the San Lorenzo Formation, dated as Middle Campanian to Early Maastrichtian [Lebrat *et al.*, 1987; Romero, 1990; Ordoñez, 1996].

Synthesizing the former data, Benítez [1995] and Jaillard *et al.* [1995] considered the Piñón Formation as early Cretaceous and identified a thin volcanic unit (Las Orquídeas Member) interlayered between the Piñón and Calentura formations. Additionally, they proposed that the evolution of southern coastal Ecuador was marked by the successive development of an eastern island arc of Coniacian-Campanian age, represented by the Cayo Formation, and a western island arc of Campanian-Maastrichtian age, corresponding to the San Lorenzo Formation. Finally, they dated as Maastrichtian to early late Paleocene the Guayaquil Formation, as well as a strongly deformed coeval series of black cherts (Santa Elena Formation), and as latest Paleocene a coarse-grained, quartz-rich conglomeratic succession (Azúcar Group).

The tectonic accretion of the Piñón terrane to the Andean margin would have occurred in the Eocene [Feininger and Bristow, 1980], Paleocene [Daly, 1989], Late Paleocene [Jaillard *et al.*, 1995; Benítez, 1995] or Late Campanian [Luzieux *et al.*, 2006].

From geochemical studies, the Piñón Formation shows affinities with oceanic plateau [Reynaud *et al.*, 1999; Lapierre *et al.*, 2000; Pourtier, 2001; Luzieux *et al.*, 2006], while the overlying magmatic or volcanoclastic successions (Las Orquídeas, Cayo and San Lorenzo Fms) exhibit island arc signatures [Lebrat *et al.*, 1987; Benítez, 1995; Reynaud *et al.*, 1999].

In the following, we shall call Calentura Formation the whole lithologic succession comprised between the Piñón Formation and the lowermost coarse-grained volcanoclastic beds of the Cayo Formation (fig. 3). The studied interval encompasses the top of the Piñón Formation, the Calentura Formation and the base of the Cayo Formation. We shall use the time scale proposed by Gradstein *et al.* [2004].

## NEW STRATIGRAPHIC DATA

### Piñón Formation

The Piñón Formation chiefly consists of olivine-free basalts and dolerites. Basalts are either massive, or pillowed, and

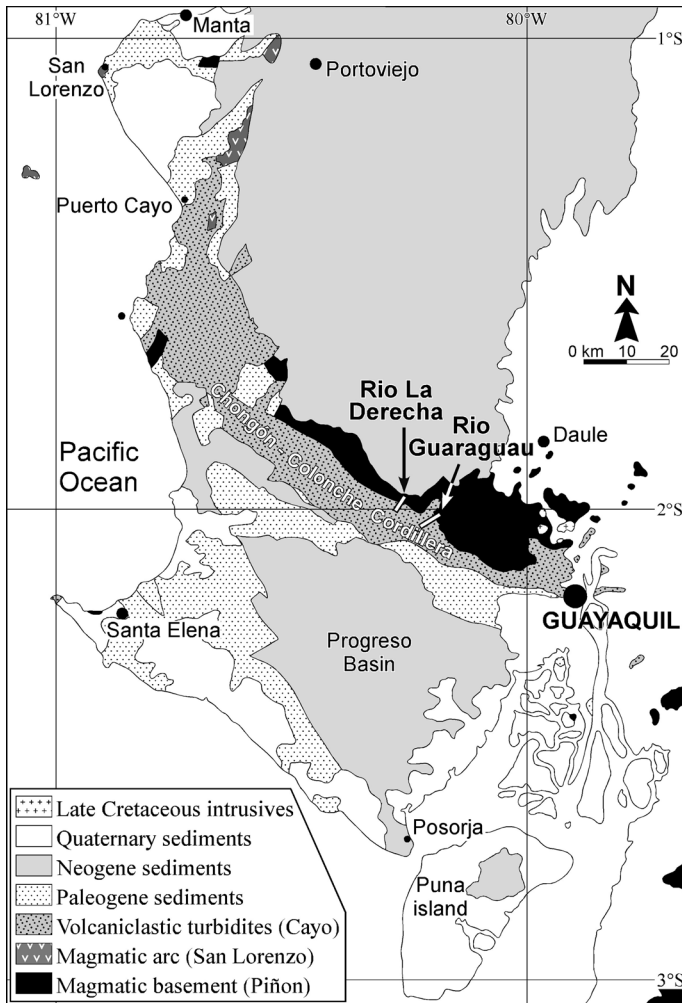


FIG. 2. – Geological sketch map of southern coastal Ecuador.  
 FIG. 2. – Carte géologique simplifiée du Sud de la côte équatorienne.

shallow level intrusions include microgabbros and ferrogabbros [Reynaud *et al.*, 1999; Pourtier, 2001].

Cherts comprised between pillows, were collected in the upper part of the unit, near the base of the Guaraguau section. They yielded the planktic foraminifera *Hedbergella holmdelensis* (Coniacian-Maastrichtian), and the radiolarians *Cryptamphorella* sp., *Orbiculiforma* sp., *Praeconocaryomma* sp., *Spongodiscus* sp., *Theocampe tina* and *Theocampe ascalia*, associated with palynomorphs (*Cicatricosisporites* sp., *Psilatricolporites* sp.).

The association of *H. holmdelensis*, *Th. ascalia* and *Th. tina* suggests an age comprised within the Coniacian-Mid Campanian interval for the Piñón Formation (fig. 3). Since the overlying Calentura Formation is of Middle Coniacian age [Ordoñez, 2007], the top of the Piñón Formation would be of Early Coniacian age. If confirmed, this data would imply that the Piñón Formation is not Early Cretaceous in age as previously assumed [Goossens and Rose, 1973; Baldock, 1982; Jaillard *et al.*, 1995; Reynaud *et al.*, 1999], and rather represents a fragment of the Caribbean Colombian Oceanic Plateau (CCOP), considered as Turonian-Coniacian in age [ $\approx$  90-85 Ma, Sinton *et al.*, 1998], as recently proposed by Luzieux *et al.* [2006].

### Calentura Formation

The Calentura Formation has been studied in the Chongón-Colonche Cordillera (CCC), West of Guayaquil, along two sections exposed along the Derecha and Guaraguau rivers, respectively (fig. 1). Although the successions are highly variable laterally, the Calentura Formation in the CCC can be tentatively subdivided into three lithologic units (fig. 3).

#### Lower unit: Volcanic breccias and limestones (Las Orquídeas Member)

This 30 to 150 m thick unit is characterized by explosive, intermediate to acidic volcanic products (58-69% SiO<sub>2</sub>). The contact with the Piñón Formation is poorly exposed. The Las Orquídeas Member includes andesitic to basaltic volcanic breccias containing porphyric andesitic fragments, scarce basaltic flows, locally brecciated (hyaloclastites), volcanoclastic debris flows, and subordinate tuffs. The breccias, pyroclastites and debris flows contain andesitic to basaltic blocks, as well as fragments of red radiolarian cherts, green tuffs and scarce limestones.

These layers are locally interbedded with thin layers of siliceous jasper, of probable hydrothermal origin, and of black siliceous limestones [Gómez and Minchala, 2003]. In the río Guaraguau section, the lower part of the section consists of laminated, organic-rich micritic limestones rich in planktic foraminifers, radiolarians and inoceramids, which grade upward into well bedded, cherty black limestones containing coarsening-upward volcanoclastic turbidites. They grade upward into radiolarian siliceous limestones, marls and tuffs (fig. 3).

The limestones contain an abundant microfauna of pelagic foraminifers and radiolarians, associated with locally abundant inoceramids. The association of the foraminifers *Dicarinella* cf. *canaliculata*, *D. cf. hagni*, *D. imbricata*, *Helvetoglobotruncana prae-helvetica*, *Whiteinella archaeocretacea*, and the radiolarian *Phaseliforma* sp., indicate a lower to mid Coniacian age [see also Velasco and Mendoza, 2003; Ordoñez, 2007]. The crushed, poorly preserved inoceramids may be either *Inoceramus* cf. *anglicus* WOODS, of Albian age, or more probably *Cremnoceramus* aff. *deformis* (MEEK) of Coniacian age (det. A. Dhondt). The lower unit of the Calentura Formation is therefore, assigned to the Middle Coniacian.

The abundance of radiolarians, planktic foraminifers and inoceramids unequivocally indicates a deep-marine, pelagic environment, probably above, and close to, the CCD, as suggested by the siliceous ribbons. The lack of any continent derived clastic input supports this interpretation, and suggests that the area was still far from any continental margin. Finally, the local occurrence of laminated, bituminous limestones indicates anoxic to dysoxic conditions.

#### Middle unit: Radiolarian cherts, arenites and debris flows

This unit rests conformably on the lower one. It is marked by the lack of volcanic activity, and the occurrence of red radiolarian cherts. It is therefore comprised between the uppermost andesitic volcanic breccia, and the lowermost tuff. According to the field sections, this unit comprises debris flows reworking andesites, tuffs and radiolarites, arkosic litharenites, litharenitic turbidites, and scarce limestones,

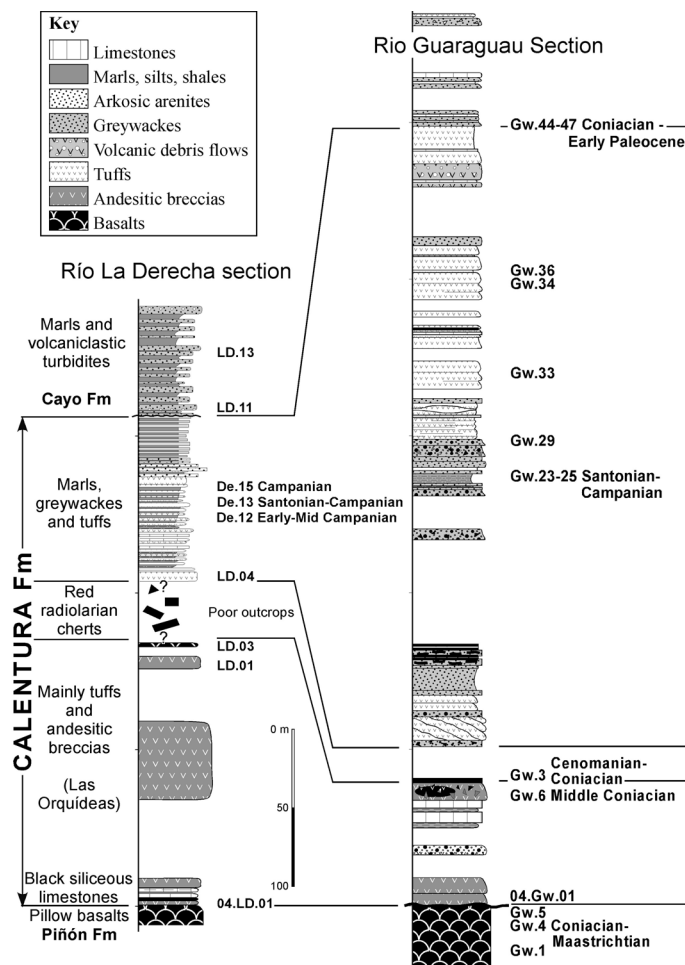


FIG. 3. – Stratigraphic sections of the Calentura Formation along the ríos La Derecha and Guaraguau.

FIG. 3. – Coupes stratigraphiques de la Formation Calentura le long des ríos La Derecha et Guaraguau.

with interbeds of red radiolarian cherts, red siliceous limestones, green shales, and arenaceous marls.

Red cherts yielded the radiolarians *Amphipyndax stocki*, *Amphisphaera* sp., *Dictyomitra* sp., *Holocryptocanium geyserense*, *Microsciadiocapsa* sp., *Obesacapsula* sp., *Phaseliforma* sp., *Protunuma* sp., *Stichomitra* sp. and *Theocampe* spp., which suggest a Cenomanian-Santonian age (fig. 3). This age is supported by the association of the foraminifers *Heterohelix* sp., *Haplophragmoides* sp. and *Whiteinella* aff. *baltica* (late Cenomanian-middle Santonian) [see also Velasco and Mendoza, 2003]. Since the basal part of the Calentura Formation is of Coniacian age, and red radiolarian cherts have been dated as Santonian-Campanian in the western Cordillera of northern Ecuador [Boland *et al.*, 2000], we ascribe this unit to the Santonian, with a probable extension into the Early Campanian.

The occurrence of exclusively pelagic microfaunas indicates deep marine, pelagic deposits. With respect to the underlying beds, this unit is marked by the abundance of siliceous cherts, and the decreasing amount of limestone beds, thus suggesting that the area, either subsided as the result of thermal subsidence due to cooling of the oceanic plateau, or experienced shallowing of the CCD. The lack of black bituminous deposits, and the dominantly red colour of

the sediments suggest a normally oxygenated environment. The presence of local clastic deposits and debris flows in the upper part suggests an uneven and moving topography, and therefore, the onset of an unstable tectonic regime.

#### Upper unit: tuffs, marls and litharenites

The base of this unit is marked by the development of thin beds of tuffs and thicker beds of welded tuffs containing abundant fragments of red cherts and red siliceous limestones. They are associated with feldspathic arenites, marls, shaly marls, commonly silicified, scarce black, siliceous micritic limestones, and coarser-grained debris flows and turbidites.

In the La Derecha and Guaraguau sections, this part of the Calentura Formation yielded a rich radiolarians assemblage including *Alievium gallowayi*, *Amphipyndax* sp., *A. stocki*, *A. pseudoconulus*, *Cryptamphorella* sp., *Diacanthocapsa* aff. *granti*, *Dictyomitra andersoni*, *D. multicostata*, *Eicyrtidium carnegiense*?, *Homeoarchicorys* sp., *Parvicuspis* cf. *shastaensis*, *Phaseliforma* sp., *Pseudoaulophacus* sp., *P. floresensis*, *P. lenticulatus*, *P. pargueraensis*, *Spongodiscus* sp. and *Stichomitra communis*, associated with scarce nannofossils (*Coccolithus* sp., *C. pelagicus*, *Micula* sp., *Watznaueria barnesae*). The association of *Amphipyndax pseudoconulus* (early to middle Campanian), *Parvicuspis* cf. *shastaensis* (Campanian), *Pseudoaulophacus lenticulatus* (middle Campanian), *P. pargueraensis* (Campanian) indicates unambiguously a Campanian age, more probably mid Campanian (fig. 3), thus confirming the conclusions of Velasco and Mendoza [2003] and Ordoñez [2007].

The disappearance of radiolarian red cherts and appearance of calcareous nannofossils can be interpreted as, either a deepening of the CCD, or an uplift of the oceanic plateau. The latter interpretation is supported by the increasing amount of volcanoclastic turbidites and coarse-grained debris flows, which suggests an increasing tectonic instability. The arkosic nature of many sandy beds indicates that the source rocks are mainly volcanics. The local occurrence of sedimentary features, comparable to those of contourites (winnowed laminae, oblique stratifications, heavy minerals concentrations), which suggest the presence of moderate currents may indicate a shallowing evolution with respect to former deposits.

#### Base of Cayo Formation

The base of the Cayo Formation is arbitrarily defined at the base of the first erosive coarse-grained turbidite bed. It is made up of graded bedded turbiditic litharenites, interbedded with sandy marls and scarce, thinly bedded tuffs, which present as a whole, a coarsening- and thickening-upward evolution.

The base of the Cayo Formation yielded benthic foraminifers (*Spiroplectammina* sp., *Bolivina* cf. *selmeensis*, *Marginulina* sp., *Epistominella* sp.), radiolarians (*Dictyomitra densicostata*, *Heliodiscus* sp., *Lithomespilus* sp., *Phaseliforma* sp., *Spongodiscus* sp.), nannofossils (*Coccolithus* sp., *Tetralithus nitidus*, *Watznaueria barnesae*), and palynomorphs (*Baltisphaeridium* cf. *sparsum*, *Dinogymnium acuminatum*, *Tricolpites* sp., *Monoletes* sp., *Echinatisporites* sp.). The co-occurrence of *Dictyomitra densicostata* (late Coniacian-Campanian) and *Tetralithus nitidus* (Campanian)

indicates a Campanian age (fig. 3). Taking into account the middle Campanian age of the underlying upper unit of the Calentura Formation, the base of the Cayo Formation must be considered as mid to late Campanian. Farther west, sedimentary beds associated with island arc suites ascribed to the Cayo or San Lorenzo formations have long been dated as Mid Campanian to Mid Maastrichtian [Sigal, 1969; Savoyat, 1971; Romero, 1990; Ordoñez, 1996; Luzieux *et al.*, 2006].

The appearance of erosional features at the base of volcanogenic turbiditic flows points to the growth of nearby reliefs. The petrography of the turbidites (litharenites with no visible quartz) suggests that these beds mainly derive from the erosion of volcanic reliefs. The Cayo Formation is therefore interpreted as a back-arc deposit, sourced by an island arc, the activity of which was announced by the tectonic instability and isolated tuffs recorded in the upper part of the Calentura Formation.

Therefore, the previous Coniacian-Campanian age assigned to the Cayo Formation [Benítez, 1995; Jaillard *et al.*, 1995] is refined. The volcanoclastic turbidites of the Cayo Formation are of Mid Campanian to younger age, and are therefore coeval with the lavas and conglomeratic debris flows of the San Lorenzo Formation of mid Campanian to mid Maastrichtian age, and can be interpreted as a distal, back-arc facies of the latter.

## PETROGRAPHY AND GEOCHEMISTRY OF VOLCANIC AND VOLCANICLASTIC ROCKS

### Analytical procedures

#### Whole rock chemistry

Major element, compatible and incompatible trace element analyses were determined by ICP – optical emission spectroscopy at the Université de Bretagne occidentale at Brest using the procedures of Cotten *et al.* [1995]. Trace elements, including the REE, were analyzed by ICP-MS at Grenoble University, after acid dissolution of 100 mg sample, using the procedures of Barrat *et al.* [1996]. Standards used for the analyses were JB2, WSE, JR1, Bir-1 and BHVO. Analytical errors are 1-3% for major-elements. Limits of detection for REE and Y = 0.03 ppm, U, Pb and Th = 0.5 ppm, Hf and Nb = 0.1 ppm, Ta = 0.03 ppm and

TABLE I. – Major element concentrations (% wt) of the Piñón Fm dolerites (GW 1, GW 5), Las Orquídeas Mb volcanic breccias (04GW-01, 04LD-01, LD 1, LD 3, GW 6) and Calentura tuffs (GW 34).

TABL. I. – *Concentration en éléments majeurs (% poids) des dolérites de la Fm Piñón (GW 1, GW 5), des brèches volcaniques du Mb Las Orquídeas (04GW-01, 04LD-01, LD 1, LD 3, GW 6) et des tufs de la Fm Calentura (GW 34).*

	Piñón Fm		Las Orquídeas Mb					Calentura
	GW1	GW5	04LD-01	04GW-01	LD1	LD3	GW6	GW34
SiO <sub>2</sub>	48.70	48.70	50.69	53.70	62.50	61.00	66.00	72.00
TiO <sub>2</sub>	1.38	1.06	0.54	1.14	0.32	0.31	0.29	0.20
Al <sub>2</sub> O <sub>3</sub>	13.20	13.40	15.95	15.23	17.25	16.70	15.05	10.15
Fe <sub>2</sub> O <sub>3</sub>	13.00	11.80	7.41	11.24	3.60	5.28	3.12	2.01
MnO	0.18	0.22	0.17	0.14	0.09	0.15	0.06	0.03
MgO	6.20	8.00	5.60	3.83	1.28	2.81	1.65	0.71
CaO	10.80	11.60	11.85	4.73	6.50	6.85	3.20	3.10
Na <sub>2</sub> O	3.15	1.71	2.65	5.21	4.65	3.70	5.11	1.56
K <sub>2</sub> O	0.05	0.09	0.37	0.93	0.36	0.33	1.89	1.14
P <sub>2</sub> O <sub>5</sub>	0.13	0.10	0.10	0.17	0.10	0.07	0.06	0.04
Loi	3.27	3.34	4.68	3.68	3.17	2.77	3.02	8.69
Total	100.06	100.02	100.00	100.00	99.82	99.97	99.45	99.63

TABLE II. – Trace element concentrations (ppm) of the Piñón Fm dolerites and basalts (GW 1, GW 5), Las Orquídeas Mb volcanic breccias (LD 1, LD 3, 04 LD 1, GW 6, 04 GW 1) and Calentura tuffs (LD 4, GW 33, GW 34, GW 36).

TABL. II. – *Concentration en éléments traces (ppm) des basaltes et dolérites de la Fm Piñón (GW 1, GW 5), des laves et brèches volcanique du Mb Las Orquídeas (LD 1, LD 3, 04 LD 1, GW 6, 04 GW 1) et des tufs de la Fm Calentura (LD 4, GW 33, GW 34, GW 36).*

	Piñón Fm		Las Orquídeas Mb					Calentura			
	GW1	GW5	04LD-01	04GW-01	LD1	LD3	GW6	LD4	GW33	GW34	GW36
Cs	0.105	0.012	0.187	0.184	0.171	0.066	0.242	0.285	0.268	0.183	0.098
Rb	5.45	0.77	12.3	10.73	3.06	3.3	23.6	13.31	15.41	15.57	9.21
Ba	112	12.1	50.2	40.6	337.8	230.3	889.2	1383.7	499	298.8	1251.7
Th	2.381	0.178	0.673	0.643	0.599	0.597	0.771	1.012	1.287	0.872	0.482
U	0.768	0.058	0.192	0.209	0.566	0.205	0.335	0.474	0.536	0.323	0.225
Nb	38.56	2.91	1.34	1.21	1.86	1.95	2.1	0.83	1.02	0.67	0.72
Ta	2.5	0.181	0.082	0.074	0.126	0.138	0.148	0.053	0.061	0.041	0.052
La	29.22	2.18	4.71	5.25	3.78	3.36	4.26	7.82	9.51	3.78	3.55
Ce	79.4	5.9	10.4	9.5	8.1	7.5	8.9	17.5	22.2	9.3	7.8
Pr	12.36	0.91	1.78	1.77	1.05	1	1.15	2.64	3.29	1.43	1.24
Pb	1.93	0.11	1.5	1.48	2.31	1.29	1.35	2.87	4.3	4.12	3.31
Nd	64.02	4.81	8.62	8.41	4.51	4.28	4.88	12.58	15.59	6.42	5.88
Sr	503	65	340	365	256	264	333	2378	535	257	1050
Sm	21.43	1.67	2.63	2.43	1.16	1.09	1.18	3.24	3.93	1.69	1.74
Zr	595.4	43.7	48.7	43.9	66.3	66.8	83.9	72.1	87.4	60.8	40.5
Hf	15.08	1.13	1.39	1.21	1.65	1.6	2.07	2.01	2.42	1.62	1.24
Eu	8.119	0.603	0.916	0.909	0.4	0.394	0.4	0.969	1.071	0.64	0.486
Gd	29.21	2.23	3.58	3.48	1.25	1.16	1.24	3.46	3.88	1.77	2.27
Tb	5.274	0.409	0.585	0.564	0.196	0.185	0.194	0.551	0.629	0.306	0.378
Dy	35.73	2.77	3.56	3.4	1.18	1.1	1.14	3.37	3.93	2.03	2.58
Ho	8.011	0.63	0.778	0.77	0.255	0.225	0.233	0.705	0.866	0.439	0.585
Er	23.42	1.81	2.35	2.19	0.74	0.65	0.65	2.18	2.61	1.37	1.82
Y	230.7	18.9	24	23.2	8	7.2	7.3	20.8	25.8	13.1	17.8
Tm			0.41	0.41							
Yb	22.64	1.74	2.87	2.91	0.68	0.62	0.62	2.14	2.64	1.42	1.82
Lu	3.42	0.266	0.409	0.412	0.113	0.098	0.094	0.316	0.387	0.232	0.292

Zr = 0.04 ppm, and less than 3% for trace elements. All the samples were pulverised in an agate mill (table I and II).

### Mineral chemistry

Major and minor elements in minerals were analyzed with a Cameca SX50 microprobe at the University of Lausanne using a 15 kV acceleration voltage and different regulated beam currents, according to the mineral type (10 nA for plagioclase, and 20 nA for olivine, pyroxenes and oxides). The calibration was made on specific natural mineral standards for each type of minerals. Trace-elements measurements on minerals were made by laser-ablation ICP-MS mass spectrometry using a 193 nm Ar-F 193 nm Lambda Physics® Excimer laser coupled with a Perkin-Elmer 6100DRC ICPMS at the University of Lausanne. NIST610 and

TABLE III. – Trace element concentrations (ppm) of clinopyroxenes from the Piñón Fm (Gw5).

TABL. III. – *Concentration en éléments traces (ppm) de clinopyroxènes de la Fm Piñón (Gw 5).*

GW5	1	2	3	4	5	6	7	8	9	10
Cs	0.009	0.003	0.004	0.002			0.003	0.002	0.002	0.005
Rb	0.07	0.03	0.02	0.08	0.03	0.04		0.1	0.01	0.07
Ba	0.2			0.2	0.1	0.1		0.2		0.1
Th			0.001		0.005	0.01	0.001		0.005	0.006
U				0.004	0.003		0.001		0.004	
Nb	0.01		0.01	0.03	0.02	0.01	0.01	0.03		0.01
Ta							0.003	0	0.001	0.009
La	0.08	0.11	0.13	0.2	0.1	0.21	0.19	0.35	0.17	0.22
Ce	0.5	0.5	0.5	0.7	0.5	0.8	0.9	1.8	0.8	0.9
Pr	0.15	0.11	0.12	0.2	0.12	0.15	0.25	0.43	0.19	0.2
Pb	0.02		0.01	0.06	0.03	0.03	0.01	0.05	0.08	0.04
Nd	0.84	0.9	1.05	1.31	0.75	1.27	1.61	3.54	1.53	1.52
Sr	4	4	4	6	4	5	5	6	5	5
Sm	0.42	0.45	0.65	0.63	0.43	0.78	1.07	1.98	0.8	0.74
Zr	2.3	2.4	2.8	4	2.3	3.4	5.7	12.3	4.3	4.6
Hf	0.13	0.08	0.24	0.22	0.09	0.14	0.33	0.68	0.3	0.24
Eu	0.153	0.153	0.177	0.213	0.155	0.274	0.332	0.671	0.283	0.271
Gd	0.94	1.03	1.11	1.02	0.78	1.2	1.75	3.3	1.33	1.65
Tb	0.152	0.137	0.231	0.185	0.129	0.243	0.314	0.635	0.233	0.253
Dy	1.32	1.16	1.37	1.55	1.33	1.56	2.68	4.89	1.84	2.05
Ho	0.24	0.265	0.33	0.334	0.243	0.434	0.536	1.04	0.454	0.495
Er	0.8	0.85	0.97	1.12	0.76	1.19	1.66	3.14	1.2	1.44
Y	6.7	6.7	7.9	9.3	6.8	10.1	14.1	26.7	10.8	11.6
Tm										
Yb	0.9	0.59	0.88	1.16	0.93	1.08	1.67	3.14	1.21	1.28
Lu	0.12	0.099	0.143	0.194	0.115	0.139	0.266	0.485	0.193	0.187

TABLE IV. – Trace element concentrations (ppm) of clinopyroxenes from the Calentura Fm (Gw 29).

TABL. IV. – Concentration en élément traces (ppm) de clinopyroxènes de la Fm Calentura (Gw 29).

GW29	1	2	3	4	5
Cs				0.001	0.001
Rb	0.02	0.01			0.04
Ba			0.1	0.1	
Th	0.001	0.002	0.005		
U	0.005				0.001
Nb		0.01			0.01
Ta	0.001				
La	1.01	0.83	0.87	0.18	0.32
Ce	5.2	4.3	4.4	0.9	1.4
Pr	1.36	1.16	1.17	0.2	0.36
Pb	0.05	0.03	0.04	0.04	0.02
Nd	10.12	9.25	9.06	1.8	2.59
Sr	19	17	17	11	12
Sm	5	4.08	4.39	0.73	1.1
Zr	11.9	9.2	9	3.1	5.7
Hf	0.62	0.51	0.43	0.19	0.36
Eu	1.26	1.206	1.029	0.213	0.347
Gd	7.44	5.81	5.29	0.88	1.63
Tb	1.146	1.086	0.962	0.203	0.284
Dy	8.64	7.62	7.25	1.49	1.88
Ho	1.832	1.595	1.413	0.332	0.409
Er	5.27	4.41	4.29	0.94	1.08
Y	44.2	36.4	37	7.9	10.3
Tm					
Yb	4.81	3.94	4.63	0.79	1.27
Lu	0.765	0.596	0.628	0.151	0.187

TABLE V. – Trace element concentrations (ppm) of clinopyroxenes from the Cayo Fm (LD 11 and LD13).

TABLE V. – Concentration en élément traces (ppm) de clinopyroxènes de la Fm Cayo (LD 11 et LD 13).

LD11	1	2	3	4	5	6	7	LD13	1	2	3	4	5	6	7	8	9
Cs				0.008	0.003	0.001	0.007		0.002	0.003	0.009	0.002	0.034			0.003	
Rb	0.01	0.02			0.01	0.02	0.03		0.02	0.03	0.01	0.04	0.06		0.03	0.03	0.03
Ba				0.1	0.8		0.5		1.7	0.2	0.1	0.5	0.1		0.1	1.1	0.4
Th	0.002		0.008			0.001	0.004		0.003	0.007	0.006	0.004	0.006	0.001	0.001		
U			0.008	0.007	0.002		0.005		0.004	0.001			0.027	0.002	0.013	0.002	0.004
Nb	0.01		0.02	0.02		0.01	0.01		0.01	0.02			0.01		0.02	0.01	
Ta		0.001		0.004	0.003	0.001			0.004		0.001				0.003		
La	0.08	0.09	0.75	0.87	0.29	0.3	0.19		0.27	0.59	0.52	0.31	0.33	0.18	0.35	0.31	0.24
Ce	0.4	0.4	3.6	4.3	1.5	1.4	1		1.3	2.6	2.4	1.4	1.6	0.9	1.2	1.5	1.3
Pr	0.1	0.11	0.89	1.13	0.43	0.38	0.26		0.29	0.63	0.62	0.36	0.4	0.23	0.32	0.46	0.36
Pb	0.01	0.01	0.02	0.07	0.03	0.02	0.04		0.02	0.05	0.09	0.07	0.04	0.01	0.05	0.14	0.04
Nd	0.68	0.78	7.33	8.88	2.87	2.67	1.99		2.32	5	4.61	2.78	2.92	1.53	2.09	3.86	2.79
Sr	21	19	13	16	13	12	12		14	14	13	12	12	13	14	15	13
Sm	0.37	0.36	3.27	4.97	1.7	1.49	1.05		1.1	2.48	2.37	1.59	1.49	0.9	1.06	1.97	1.56
Eu	1.6	1.7	10.7	12.9	4	3.9	3.7		3.8	9	7.9	5.6	6.3	2.7	3.3	5.3	4.9
Hf	0.11	0.11	0.65	0.71	0.28	0.24	0.15		0.16	0.48	0.43	0.36	0.39	0.13	0.15	0.35	0.24
Eu	0.224	0.178	0.841	1.151	0.424	0.518	0.379		0.393	0.611	0.556	0.405	0.445	0.267	0.338	0.505	0.434
Gd	0.6	0.55	5.78	7.88	2.36	2.43	1.58		1.84	3.57	3.99	2.26	2.79	1.34	1.65	2.55	2.23
Tb	0.113	0.109	1.115	1.359	0.446	0.44	0.349		0.322	0.712	0.754	0.462	0.494	0.235	0.262	0.515	0.423
Dy	0.84	0.73	8.64	10.35	3.28	3.35	2.8		2.31	5.52	5.13	3.4	3.88	1.69	2.32	3.82	3.31
Ho	0.145	0.147	1.922	2.337	0.728	0.753	0.606		0.484	1.195	1.059	0.722	0.829	0.346	0.479	0.761	0.723
Er	0.41	0.42	5.34	6.43	2.09	2.09	1.42		1.44	3.55	3.43	2.23	2.55	1.15	1.29	2.21	1.85
Y	3.4	3.5	41.6	54.2	17.5	16.5	13		11.6	28.4	27.7	18.6	20.3	9	11.4	19.2	15.3
Tm																	
Yb	0.45	0.37	4.72	5.7	1.99	1.94	1.54		1.16	3.31	2.95	2.09	2.49	0.91	1.23	2.09	1.83
Lu	0.042	0.038	0.693	0.806	0.254	0.28	0.224		0.182	0.501	0.433	0.333	0.377	0.151	0.197	0.323	0.234

612 glasses were used as external standards, Ca and Si as internal standards after microprobe measurements on the pit sites. Ablation pit size varied from 40 to 60  $\mu\text{m}$ . BCR2 basaltic glass was regularly used as a monitor to check for reproducibility and accuracy of the system. Results were always within  $\pm 10\%$  of the certified values (table III to VI).

### Piñón Formation (Turonian? - Coniacian)

The pillow basalts of the Piñón Formation exhibit intersertal textures formed of plagioclase laths embedded in subhedral clinopyroxene phenocrysts. Plagioclase and clinopyroxene crystals varie in size from 3 to 0.5 mm. The smallest crystals exhibit quenched textures. The interstitial groundmass

includes late crystallizing acicular or cubic oxides (titano-magnetite, local quenched textures). The crystal sequence of these basalts (plagioclase  $\rightarrow$  clinopyroxene  $\rightarrow$  Fe-Ti oxides) is typical of tholeiites.

Clinopyroxene major element chemistry is that of an augite (Wo 38-45, En 37-43, Fs 14-24; fig. 4A). Plagioclase is generally altered (replaced by albite) but when preserved, has a bytownite-labradorite composition (An 70%; fig. 4B). Clinopyroxene chondrite-normalized [Sun and McDonough, 1989] (fig. 5) rare earth patterns (REE) are very similar and do not show differences between core and rim of a single crystal or between crystals. They are light (L)REE-depleted and show marked negative Eu anomalies. The REE abundances range between 1 to 5 times the chondritic abundances.

With respect to major and trace element chemistry, the Piñón lavas show features of oceanic plateau basalts [Kerr *et al.*, 1996], *i.e.* MgO = 6-7%, TiO<sub>2</sub> = 1,5%, chondrite-normalized (fig. 6) rare earth flat patterns, primitive mantle-normalized (fig. 6) multi-element plot characterized by positive Eu and Sr anomalies, and absence of Nb and Ta negative anomalies (La/Nb < 1)

### Volcanics of the lower Calentura Formation (Las Orquídeas Member, Coniacian)

Lavas from the Las Orquídeas member were sampled in the matrix of the volcanic breccias. They are mostly porphyritic

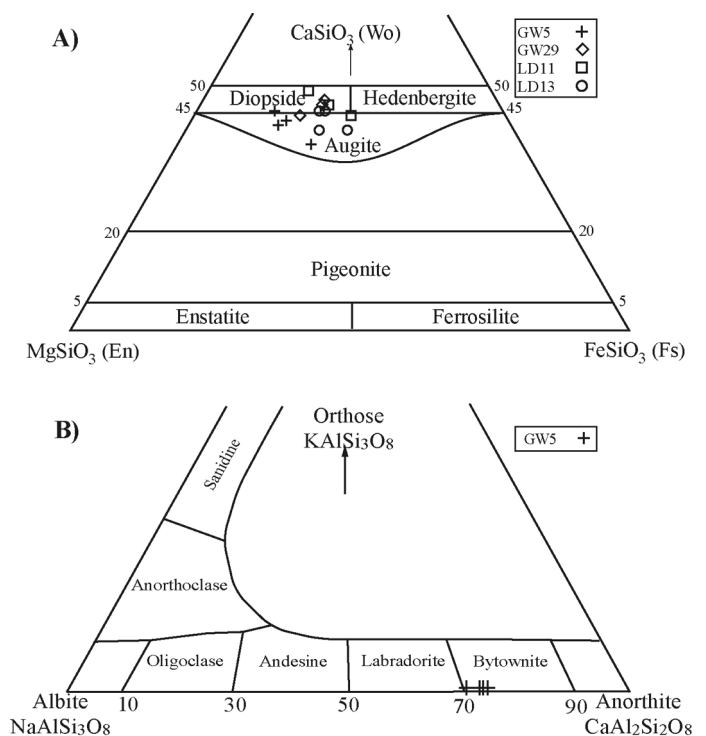


FIG. 4. – A) Composition diagram of clinopyroxenes of the Piñón (GW 5) and Calentura (GW 29, LD 11, LD 13) formations. Sample location on figure 3.

B) Composition diagram of feldspars of the Piñón Formation (GW 5). Sample location on figure 3.

FIG. 4. – A) Composition des clinopyroxènes des formations Piñón (GW 5) et Calentura (GW 29, LD 11, LD 13). Localisation des échantillons sur la figure 3.

B) Composition des feldspaths de la Formation Piñón (GW 5). Localisation des échantillons sur la figure 3.

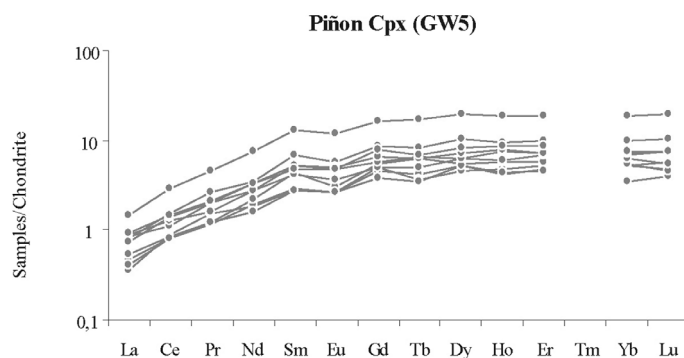


FIG. 5. – Rare earth element composition of 10 clinopyroxenes from the Piñón Formation (GW 5), normalized to chondrite [Sun and Mc Donough, 1989]. Data on table III.

FIG. 5. – Composition en terres rares de 10 clinopyroxènes de la formation Piñón (GW 5), normalisée aux chondrites [Sun and Mc Donough, 1989]. Données dans le tableau III.

rocks with an high mesostase content (40%), made up of plagioclase microliths, or monocrystals of pyroxene, plagioclase and oxides. However, the mineralogy, crystallization sequence and geochemistry differ from base to top.

Near the base of the unit (04GW-01 and 04LD-01), the clinopyroxene phenocrysts dominate, they postdate the plagioclase, and do not include oxide crystals, thus indicating the following crystallization sequence: plagioclase  $\Rightarrow$  clinopyroxènes  $\Rightarrow$  Fe-Ti oxides. These lavas have moderate Mg content ( $3.83 < \text{MgO}\% < 5.6$ ), and the rare earth elements (REE) diagram normalized to chondrites (fig. 6) exhibits a flat pattern ( $(\text{La}/\text{Yb})_n \approx 1.2$ ). Nevertheless, multi-elementary diagrams, normalized to primitive mantle (fig. 6), exhibit negative anomalies for Nb and Ta for all rocks, evidencing a magmatic arc origin for all samples from this unit.

In the upper part of this member (GW6, LD1 and LD3), plagioclases are abundant and are usually grouped into glomerophytic aggregates, and oxides are included into plagioclase and pyroxene crystals, indicating the early growth of oxides. These lavas have low Mg content ( $1.3 < \text{MgO}\% < 1.9$ ), are moderately alkaline ( $5.18 < \text{Na}_2\text{O} + \text{K}_2\text{O} < 7.26$ ), and show high Si contents ( $\text{SiO}_2 > 60\%$ ), displaying features of andesites or dacites. The REE plot normalized to chondrites (fig. 6) exhibit Light REE enrichment, and a flat pattern for heavy REE ( $3.9 < (\text{La}/\text{Yb})_n < 5$ ).

The chemical differences between the base and top of this member are interpreted as due to the decreasing abundance of pyroxene. Comparison with the tuffs of the upper part of the Calentura Formation leads to interpret the lavas of the Las Orquídeas Member as tholeiitic arc lavas, which evolve to a calc-alkaline series through time, as already proposed by Reynaud *et al.* [1999].

#### Tuffs of the upper Calentura Formation (mid Campanian)

Tuffs of the upper part of the Calentura Formation are marked by a very high matrix content (50 to 60% of whole rock). The matrix is mainly formed of very fine ash or of chards of volcanic glass, which present flow features. These rocks contain sedimentary clasts, especially red radiolarian cherts, and few crystals, among which some fragments of

pyroxenes are associated with two plagioclases: small sized albites exhibiting oxide inclusions and larger, crackled calcic plagioclases. This texture confirms an explosive emplacement. The grain size of these clasts decreases from base to top.

Trace elements concentration in the tuffs is typical of island arc volcanism. Multi-elemental diagrams normalized to primitive mantle (fig. 6) show a negative anomaly in Nb and Ta. Chondrite normalized REE diagrams are marked by a negative anomaly in Eu and a moderate enrichment in heavy REE ( $1.4 < (\text{La}/\text{Yb})_n < 2.6$ ). Since Reynaud *et al.* [1999], found similar characteristics in the San Lorenzo lavas (fig. 6), the tuffs of the upper Calentura Formation are interpreted as products of an island arc.

#### Lower Cayo Formation (mid to late Campanian)

Because the Cayo Formation only contains volcanoclastic sediments (greywackes), we only analyzed pyroxene considered representative of the source area. We included in this section the sample GW 29 from the Calentura Formation, since it does not differ significantly from those of the Cayo Formation. Pyroxenes of the Cayo Formation (samples GW 29, LD 11 and LD13; fig. 4A) are either augites (Wo 40-47, En 28-37, Fs 19-29), or diopsides (Wo 47-49, En 31-33, Fs 19-22). Their chondrite-normalized spider diagrams (fig. 7) show a depletion in L-REE, although this depletion is less marked for two pyroxenes of sample LD 11. The most depleted crystals are marked by a positive anomaly in Eu, while the others present a negative anomaly in the same element. The latter feature is interpreted as the result of the early crystallization of clinopyroxene (clinopyroxene  $\rightarrow$  plagioclase  $\rightarrow$  Fe-Ti oxydes) and conversely, the early crystallization of oxides characterizes calc-alkaline series. Therefore, our results confirm the interpretations proposed by Benítez [1995], who assumed that the litharenitic turbidites of the Cayo Formation derive from an active and partially emergent island arc.

#### GEODYNAMIC INTERPRETATIONS AND DISCUSSIONS

In the following discussion, the tectonic unit formed by the Piñón Formation and its overlying stratigraphic succession will be referred to as the Piñón terrane. Our new data on the stratigraphy of the Calentura and Cayo formations show that on one hand, the Piñón terrane was part of the Caribbean Plateau, and on the other hand, the San Lorenzo and Cayo formations represent the proximal and distal facies, respectively of a single island arc of Mid Campanian – Mid Maastrichtian age. The pre-collision evolution of the Piñón terrane can be reconstructed as follows (fig. 8).

About 90 Ma ago (Turonian?-Coniacian), the Piñón Formation was created by a mantle plume in the paleo-Pacific ocean, as part of the Caribbean Colombian Oceanic Plateau (CCOP).

Between  $\approx 90$  and 88 Ma (Early Coniacian), *i.e.* immediately after the birth of the oceanic plateau, volcanic breccias and lavas (Las Orquídeas Mb) are emplaced on top of this part of the CCOP. Although these volcanic rocks exhibit a tholeiitic island arc signature, a geodynamic context involving an active arc in this region at that time is unlikely for three main reasons. First, the genesis of island arc lavas

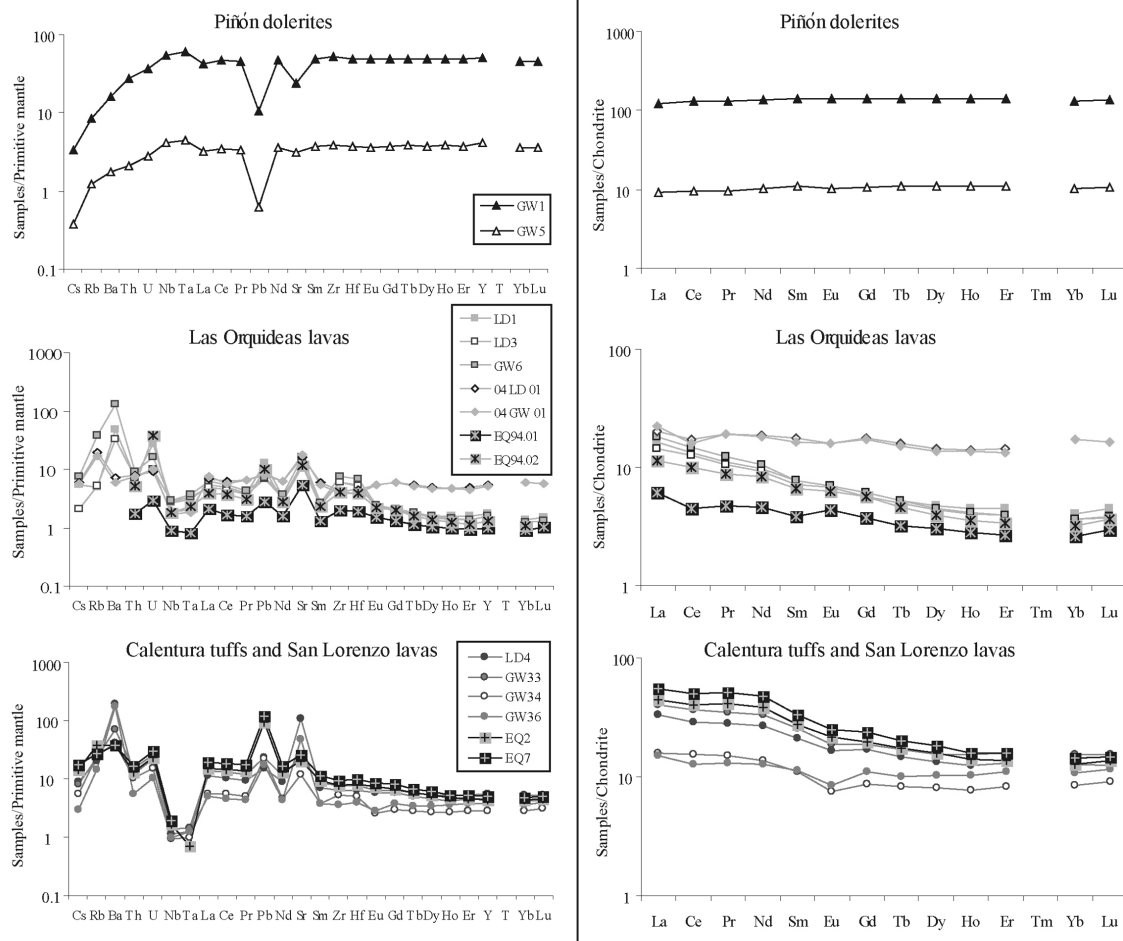


FIG. 6. – Trace elements composition normalized to primitive mantle, and rare earth elements composition normalized to chondrite [Sun and Mc Donough, 1989], of the Piñón Formation (above), Las Orquídeas Member (center) and Calentura tuffs (below). Data on table II. San Lorenzo arc lavas (EQ 2, EQ 7) and Las Orquídeas lavas (EQ94-01 and EQ94-02) from Reynaud *et al.* [1999].

FIG. 6. – Compositions en éléments traces normalisées au manteau primitif, et compositions en terres rares normalisées aux chondrites [Sun and Mc Donough, 1989], de la formation Piñón (haut), du membre Las Orquídeas (milieu) et des tufs de la formation Calentura (bas). Données dans le tableau II. Laves de l'arc San Lorenzo (EQ 2, EQ 7) et de Las Orquídeas (EQ94-01 et EQ94-02) d'après Reynaud *et al.* [1999].

requires that a subducting oceanic lithosphere reached the depth of magma genesis ( $\approx 100$  km). However, it is difficult to assume that about 150 km of oceanic lithosphere had been subducted, and that the generated magma ascends to the surface in such a short time ( $\approx 2$  Ma). Second, magmatic island arc activity is usually abundant, yet the Las Orquídeas Member is only 20 to 200 m thick. Finally, assuming that oceanic subduction began immediately beneath the newly created oceanic plateau and produced the Las Orquídeas lavas, it seems quite unlikely that subduction then ceased after Early Coniacian ( $\approx 88$  Ma) before to resume by Mid Campanian times ( $\approx 80$  Ma) to produce the overlying Cayo and San Lorenzo formations (fig. 8).

Although speculative, we therefore propose that the Las Orquídeas Member was originated by partial melting of deep parts of the CCOP. In that interpretation, the magmatic source would be rich in ilmenite, and in amphiboles altered by hydrothermal process, as proposed by Haase *et al.* [2005] for arc-like lavas associated with mid-ocean ridges. Note that Allibon *et al.* [2005] also stressed the influence of the still hot CCOP in the contamination and Mg-enrichment of the Mid Campanian island arc lavas in Ecuador, thus

supporting the input of the hot roots of oceanic plateaus in the genesis of subsequent magmatism. Furthermore, partial melting of the plateau crust has been proposed to explain tonalitic intrusions dated at 85-82 Ma in Aruba [White *et al.*, 1999]. A similar origin could be invoked for the Pujilí granite in Ecuador, recently dated at 86 Ma [Spiking *et al.*, 2005; Vallejo *et al.*, 2006].

During the Middle to Late Coniacian ( $\approx 88 - 86$  Ma), black, organic-rich siliceous limestones were deposited above the CCD, maybe during the anoxic oceanic event identified in the Late Coniacian-Early Santonian [Jenkyns *et al.*, 1980; Arthur *et al.*, 1988; Wagner, 2002]. The lack of any magmatic activity suggests that no subduction occurred at that time, and therefore, that the Piñón terrane belonged to the paleo-Pacific plate and migrated passively with it (fig. 8). During the Santonian-Early Campanian ( $\approx 86 - 80$  Ma), deposition of red, radiolarian rich cherts indicates that this part of the CCOP subsided below the CCD. This change is tentatively interpreted as due to thermal subsidence related to plateau cooling.

The Middle Campanian – Early Maastrichtian time span ( $\approx 80 - 71$  Ma) is marked first by the deposition of deep

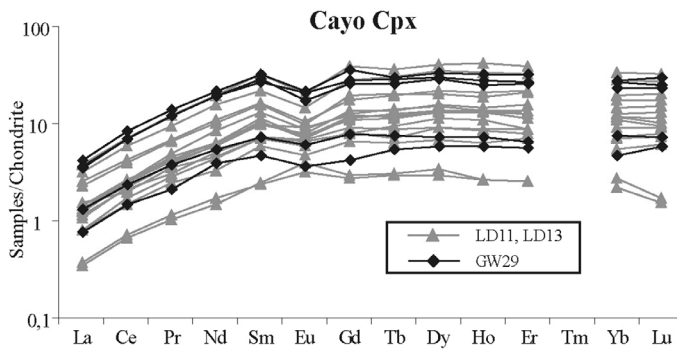


FIG. 7. – Rare earth elements composition of 12 clinopyroxenes of the Cayo Formation, normalized to chondrite [Sun and Mc Donough, 1989]. Sample location on figure 3, data on table IV and V.  
 FIG. 7. – Concentration en terres rares des clinopyroxènes de la formation Cayo, normalisée aux chondrites [Sun and Mc Donough, 1989]. Localisation des échantillons sur la figure 3, données sur les tableaux IV et V.

marine marls and arenites, and incipient development of an island arc (tuffs), then giving way to the deposition of thick volcanoclastic turbidites (Cayo Fm) that reworked an active island arc, presently located farther west (San Lorenzo Fm). The disappearance of radiolarian rich calcareous cherts in the Middle Campanian suggests that the plateau surface was uplifted, as suggested by evidences of tectonic activity (detrital input, reworking of red radiolarian cherts) and the occurrence of subaerial volcanism. The onset of an island arc activity unambiguously indicates the creation of a subduction beneath the Piñón terrane. Taking into account the 60 – 90° clockwise rotation undergone by the Piñón terrane [Roperch *et al.*, 1987; Luzieux *et al.*, 2006] and the present-day

west location of the San Lorenzo island arc to the west, the subduction zone was probably located at the southern tip of the COP. From then on, the Piñón terrane, and possibly the whole CCOP, were therefore individualized as an oceanic plate, independent from the paleo-Pacific plate.

From Mid Maastrichtian ( $\approx 68$  Ma) to early Late Paleocene (Mid Thanetian;  $\approx 58$  Ma), the Piñón terrane received pelagic, radiolarian-rich, black siliceous cherts (Guayaquil Fm), without any continent deriving detrital input (fig. 8). However, an eastern part of the CCOP is proved to have been in contact with the Ecuadorian continental margin in the Late Maastrichtian (Guaranda terrane of the Western Cordillera of Ecuador) [Jaillard *et al.*, 2004], whereas the Piñón terrane received unconformable detrital quartz as late as in the Late Paleocene ( $\approx 58$  Ma). If the Piñón terrane actually was a part of the CCOP, this implies that the CCOP had been splitted into at least two independent tectonic units: (1) an eastern terrane accreted to the margin in the Late Maastrichtian (Guaranda terrane), and (2) a western one (Piñón terrane), which remained preserved from continent deriving clastic input, until it was accreted to the former in the Late Paleocene. In this interpretation, the Late Paleocene accretion would represent the collision and underthrusting of the Piñón terrane beneath the Guaranda terrane that was already part of the Andean margin.

## CONCLUSIONS

The study of the stratigraphic succession of the Piñón terrane made it possible to ascribe the Piñón terrane to the CCOP, to demonstrate the time-equivalence of the Cayo and San Lorenzo arc of southern Coastal Ecuador, and to

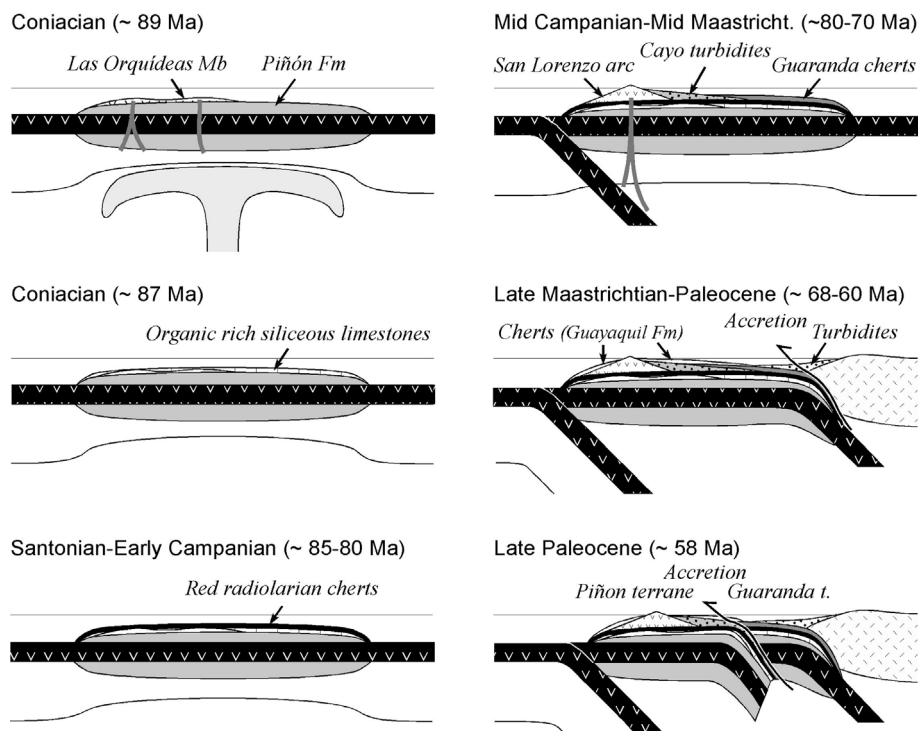


FIG. 8. – Proposed scenario for the geodynamic evolution of the CCOP (Piñón and Guaranda terranes) between Coniacian and Paleocene times.  
 FIG. 8. – Scénario proposé pour l'évolution géodynamique du CCOP (terrains Piñón et Guaranda) entre le Coniacien et le Paléocène.

propose a reconstruction of its pre-collision and accretionary evolution.

The pre-accretion evolution is marked by an early and ephemeral volcanic activity (early Coniacian), tentatively interpreted as the result of partial melting of the base of the CCOP. This is followed by oceanic sedimentation at depths close to the CCD (Santonian, early Campanian?), and then by the creation of a subduction zone beneath this part of the CCOP (Mid Campanian). This major event individualized the CCOP as an oceanic plate independent from the paleo-Pacific oceanic plate.

Although part of the CCOP is known to have been accreted to the Ecuadorian margin in the Late Maastrichtian (Guaranda terrane), the Piñón terrane still received oceanic deposits devoid from any continent derived clastic input until the early Late Paleocene. This suggests that the Piñón

terrane was far away from the Guaranda terrane and/or was sheltered from continent derived clastics by a sedimentary trap. In the Late Paleocene, the Piñón terrane eventually was underthrust beneath the already accreted Guaranda part of the CCOP, thus splitting the Ecuadorian part of the CCOP into two terranes (Guaranda to the east, and Piñón to the west).

*Acknowledgements.* – This paper is dedicated to our friend and colleague, Prof. Henriette Lapiere who died abruptly on January 14th, 2006 in Syria. Special thanks are due to Dr. Annie Dhondt (Bruxelles), deceased in September 2006, who studied the inoceramids. We are indebted to the Institut de Recherche pour le Développement (IRD, France), which supported financially this project, to Petroproducción (Ecuador), which allowed publication of these results, to J. Allibon (Lausanne), who revised the English text, to L. Luzieux (Zürich) and R. Spikings (Geneva) for animated and constructive discussions, and to Y. Lagabrielle (Montpellier) and J. Hernandez (Lausanne) for their thorough revision of this text.

## References

- ALLIBON J., LAPIERRE H., JAILLARD E., MONJOIE P., BUSSY F. & BOSCH D. (2005). – High Mg-basalts in the western Cordillera of Ecuador: Evidence of plateau root melting during Late Cretaceous arc-magmatism. – *6th ISAG*, Barcelona 2005, Extend. Abst. Vol., 33-35.
- ARTHUR M.A., JENKINS H.C., BRUMSACK H.J. & SCHLANGER S.O. (1988). – Stratigraphy, geochemistry, and paleo-oceanography of organic carbon-rich Cretaceous sequences. In: R.N. GINSBURG & B. BEAUDOUIN, Eds., *Cretaceous resources, events and rhythms*, Background and plans for research. – *NATO ASI Series*, Kluwer, Dordrecht, 75-120.
- BALDOCK J.W. (1982). – Geología del Ecuador. – *Boletín de Explicación del Mapa geológico de la República del Ecuador*. Dirección General de Geología y Minas, Quito, 70 p.
- BARRAT J.A., KELLER F. & AMOSSE J. (1996). – Determination of rare earth elements in sixteen reference samples by ICPMS after addition and ion exchange separation. – *Geostand. Newslett.*, **20**, 133-139.
- BENÍTEZ S. (1995). – Evolution géodynamique de la province côtière sud-équatorienne au Crétacé supérieur-Tertiaire. – *Géol. Alpine*, **71**, 3-163.
- BOLAND M.P., MCCOURT W.J. & BEATE B. (2000). – Mapa geológico de la Cordillera occidental del Ecuador entre 0°-1°N, escala 1/200.000. – Minist. Energ. Min.-BGS publs., Quito.
- BRISTOW C.R. (1976). – The age of the Cayo Formation, Ecuador. – *Newsl. Stratigr.*, **4**, 169-173, Stuttgart.
- COTTEN J., LE DEZ A., BAU M., CAROFF M., MAURY R.C., DULSKI P., FOURCADE S., BOHN M. & BROUSSE R. (1995). – Origin of anomalous rare earth elements and yttrium enrichments in subaerially exposed basalts: Evidence from French Polynesia. – *Chem. Geol.*, **119**, 115-138.
- DALY M.C. (1989). – Correlations between Nazca/Farallón plate kinematics and forearc basin evolution in Ecuador. – *Tectonics*, **8**, 769-790.
- FAUCHER B. & SAVOYAT E. (1973). – Esquisse géologique des Andes de l'Equateur. – *Rev. Géogr. Phys. Géol. Dyn.*, (2), **15**, 115-142, Paris.
- FEININGER T. & BRISTOW C.R. (1980). – Cretaceous and Paleogene history of coastal Ecuador. – *Geol. Rundsch.*, **69**, 849-874.
- GANSSE A. (1973). – Facts and theories on the Andes. – *J. Geol. Soc.*, London, **129**, 93-131.
- GÓMEZ H.E. & MINCHALA G.J. (2003). – Estudio estratigráfico de la Formación Calentura, sector Pedro Carbo. Implicaciones hidrocarbúferas. – Thesis Ing. Esc. Sup. Politecn. Litoral, Guayaquil, 293 p.
- GOOSSENS P.J. & ROSE W.I. (1973). – Chemical composition and age determination of tholeiitic rocks in the basic Cretaceous Complex, Ecuador. – *Geol. Soc. Amer. Bull.*, **84**, 1043-1052.
- GOOSSENS P.J., ROSE W.I. & FLORES D. (1977). – Geochemistry of tholeiites of the Basic Igneous Complex of northwestern South America. – *Geol. Soc. Amer. Bull.*, **88**, 1711-1720.
- GRADSTEIN F.M., OGG J.G. & SMITH A.G. (2004). – A geological time scale. – Cambridge Univ. Press., 589 pp.
- HAASE K.M., STRONCIK N.A., HEKINIAN R. & STOFFERS P. (2005). – Nb-depleted andesites from the Pacific-Antarctic Rise as analogs for early continental crust. – *Geology*, **33**, 921-924.
- JAILLARD E., ORDONEZ M., BENITEZ S., BERRONES G., JIMENEZ N., MONTENEGRO G. & ZAMBRANO I. (1995). – Basin development in an accretionary, oceanic-floored forearc setting: southern coastal Ecuador during late Cretaceous to late Eocene times. In: A.J. TANKARD, R. SUAREZ & H.J. WELSINK, Eds., *Petroleum basins of South America*. – *Am. Ass. Petrol. Geol. Mem.*, **62**, 615-631.
- JAILLARD E., ORDONEZ M., SUAREZ J., TORO J., IZA D. & LUGO W. (2004). – Stratigraphy of the late Cretaceous-Paleogene deposits of the Cordillera Occidental of central Ecuador: Geodynamic implications. – *J. South Am. Earth Sci.*, **17**, 49-58.
- JENKINS H.C. (1980). – Cretaceous anoxic events: from continents to oceans. – *J. Geol. Soc. London*, **137**, 171-188.
- KERR A.C., TARNEY J., MARRINER G.F., NIVIA A. & SAUNDERS A.D. (1996). – The geochemistry and tectonic setting of Late Cretaceous Caribbean and Colombian volcanism. – *J. South Am. Earth Sci.*, **9**, 111-120.
- KERR A.C., ASPDEN J.A., TARNEY J. & PILATASIG L.F. (2002). – The nature and provenance of accreted terranes in western Ecuador: Geochemical and tectonic constraints. – *J. Geol. Soc., London*, **159**, 577-594.
- KERR A.C. & TARNEY J. (2005). – Tectonic evolution of the Caribbean and northwestern South America: The case for accretion of two Late Cretaceous oceanic plateaus. – *Geology*, **33**, 269-272.
- LAPIERRE H., BOSCH D., DUPUIS V., POLVE M., MAURY R.C., HERNANDEZ J., MONIE P., YEGHICHEYAN D., JAILLARD E., TARDY M., MERCIER DE LEPINAY B., MAMBERTI M., DESMET A., KELLER F. & SENEBIER F. (2000). – Multiple plume events in the genesis of the peri-Caribbean Cretaceous oceanic plateau Province. – *J. Geophys. Res.*, **105**, 8 403-8 421.
- LEBRAT M., MEGARD F., DUPUY C. & DOSTAL J. (1987). – Geochemistry and tectonic setting of pre-collision Cretaceous and Paleogene volcanic rocks of Ecuador. – *Geol. Soc. Amer. Bull.*, **99**, 569-578.
- LUZIEUX L., HELLER F., SPIKINGS R., VALLEJO C. & WINKLER W. (2006). – Origin and Cretaceous history of the coastal Ecuadorian forearc between 1°N and 3°S: paleomagnetic, radiometric and fossil evidence. – *Earth Planet. Sci. Lett.*, **249**, 400-414.

- MAMBERTI M., LAPIERRE H., BOSCH D., JAILLARD E., ETHIEN R., HERNANDEZ J. & POLVE M. (2003). – Accreted fragments of the Late Cretaceous Caribbean-Colombian Plateau in Ecuador. – *Lithos*, **66**, 173-199.
- MAMBERTI M., LAPIERRE H., BOSCH D., JAILLARD., HERNANDEZ J. & POLVE M. (2004). – The Early Cretaceous San Juan plutonic Suite, Ecuador: A magma chamber in an oceanic plateau? – *Can. J. Earth Sci.*, **41**, 1237-1258.
- MARKSTEINER R. & ALEMAN A. (1991). – Coastal Ecuador. Technical evaluation agreement. – Amoco Prod. Co & Petroecuador, Internal report, 1, 218 p.
- OLSSON A.A. (1942). – Tertiary deposits of northwestern South America and Panama. – *Proc. 8th Am. Sci. Congr.*, **4**, 231-287, Washington.
- ORDOÑEZ M. (1996). – Aplicaciones del estudio de microfósiles en la industria petrolera ecuatoriana. – *Actas VII Cong. Ecuat. Geol. Min. Petrol.*, 38-52, Quito.
- ORDOÑEZ M. (2007). – Asociaciones de radiolarios de la cordillera Chongón-Colonche, Ecuador (Coniaciano-Eoceno). – 4th European Meeting on the paleontology and stratigraphy of Latin America, Extend. Abstract. – *Cuadernos Museo Geominero*, **8**, 291-299, Madrid.
- POURTIER E. (2001). – Pétrologie et géochimie des unités magmatiques de la côte équatorienne: implications géodynamiques. – DEA thesis, Univ. Aix-Marseille, 35 p.
- REYNAUD C., JAILLARD É., LAPIERRE H., MAMBERTI M. & MASCLE G.H. (1999). – Oceanic plateau and island arcs of southwestern Ecuador: their place in the geodynamic evolution of northwestern South America. – *Tectonophysics*, **307**, 235-254.
- ROMERO J. (1990). – Estudio estratigráfico detallado de los acantilados de Machalilla, Provincia de Manabí. – Tesis Ing. Geol., Esc. Sup. Pol. Lit., Guayaquil, 259 p.
- ROPERCH P., MEGARD F., LAJ C., MOURIER T., CLUBE T. & NOBLET C. (1987). – Rotated oceanic blocks in western Ecuador. – *Geophys. Res. Lett.*, **14**, 558-561.
- SAVOYAT E. (1971). – Mapa y leyenda explicativa de la hoja de Manta al 1/100.000. – Dir. Gen. Geol. Minas, Minist. Recurs. Natur. Turismo, Quito.
- SIGAL J. (1969). – Quelques acquisitions récentes concernant la chrono-stratigraphie des formations sédimentaires de l'Équateur. – *Rev. Española Micropaleont.*, **1**, 205-236.
- SINTON C.W., DUNCAN R.A., STOREY M., LEWIS J. & ESTRADA J.J. (1998). – An oceanic flood basalt province within the Caribbean plate. – *Earth Planet. Sci. Lett.*, **155**, 221-235.
- SPIKING R., WINKLER W., HUGHES R.A. & HANDLER R. (2005). – Thermochronology of allochthonous terranes in Ecuador: unraveling the accretionary and post-accretionary history of the northern Andes. – *Tectonophysics*, **399**, 195-220.
- SUN S.S. & McDONOUGH W.F. (1989). – Chemical and isotopic systematics of ocean basalts: implications for the mantle compositions and processes. In: A.D. SAUNDERS, M.G. NORY, Eds. Magmatism in ocean basins. – *Geol. Soc. Lond. Spec. Pub.*, **42**, 313-345.
- THALMANN H.E. (1946). – Micropaleontology of Upper Cretaceous and Paleocene in western Ecuador. – *Am. Ass. Petrol. Geol. Bull.*, **30**, 337-347.
- VALLEJO C., SPIKINGS R.A., LUZIEUX L., WINKLER W., CHEW D. & PAGE L. (2006). – The early interaction between the Caribbean Plateau and the NW South American Plate. – *Terra Nova*, **18**, 264-269.
- VELASCO S. M-L. & MENDOZA I.K. (2003). – Estudio geológico del Miembro Calentura de la Formación Cayo en el flanco oriental de la Cordillera Chongón-Colonche. – Thesis Ing. Univ. Guayaquil, 182 pp., unpubl.
- WAGNER T. (2002). – Late Cretaceous to early Quaternary organic sedimentation in eastern Equatorial Atlantic. – *Palaeogeogr., Palaeoclimatol., Palaeoecol.*, **179**, 113-147.
- WHITE R.V., TARNEY J., KERR A.C., SAUNDERS A.D., KEMPTON P.D., PRINGLE M.S. & KLAVER G.T. (1999). – Modification of an oceanic plateau, Aruba, Dutch Caribbean: Implications for the generation of continental crust. – *Lithos*, **46**, 43-68.